DEVELOPING A METHOD FOR DETERMINING THE NATURAL FREQUENCY OF A STRUCTURE USING MULTIPLE COMBINED MEASUREMENTS IN THE FREQUENCY DOMAIN

VU DINH HUONG[a,*], **TA DUC TUAN**[a]
[a]Le Quy Don Technical University
[*]Corresponding author: *email: vudinhhuong@lqdtu.edu.vn*

Abstract: *Modal identification of structures using vibration measurement data has attracted considerable attention. Current identification methods can be divided into several groups: single-degree-of-freedom and multi-degrees-of-freedom methods; time domain identification, frequency domain identification. In which, the simultaneous determination of many natural frequencies of the structure from a single measurement data remains a complicated problem, in particular in the presence of noise. The article develops the rational fraction polynomial method using combined measurements in the frequency domain to identify the natural frequencies of structures. The effectiveness of the proposed method is validated by numerical simulations and experimental tests of steel beam.*

Keywords: *Natural frequency identification, rational fraction polynomial method, vibration measurement, noise, frequency domain.*

1. Introduction

Modal analysis is a rather complex problem in engineering mechanics. In particular, the determination of the natural frequency of the structure is a matter of interest to many scientists. Current methods can be divided as follows: single-degree-of-freedom (SDOF) identification, multi-degrees-of-freedom (MDOF) identification; time domain identification, frequency domain identification.

There are many popular methods in the time domain, such as Ibrahim Time Domain [1], Complex Exponential (CE) [2] or Least Squares Complex Exponential (LSCE) [3]. Ibrahim et al. [1] proposed a method to determine the natural frequency in the time domain from the free response of structures. The authors used the least squares (LS) procedure and a mathematical model with more degrees of freedom than the number of needed modes to remove noise in higher-order modes. The CE method introduced by

Spitznogle [2] uses impulse response functions (IRFs). The advantage of the CE method is its simplicity, requiring only one measurement to determine the natural frequencies. However, this method is sensitive to measurement noise and requires knowing a number of modes in advance. The LSCE method [3] uses multiple IRF measurements simultaneously to determine the natural frequencies and damping ratios. This method uses the LS procedure for many measured data, which overcomes the CE method's sensitivity to noise.

Frequency domain methods are often used to determine the dynamic characteristics of structures. Among these methods, there is a group based on SDOF and a group based on MDOF. SDOF based methods: Peak-picking method, Circle-Fit method; Inverse method [4]; integral method [5]. The Peak-Picking is a simple method and is widely used to identify modal parameters of structures [6-10]. This method assumes that the frequency response function (FRF) of a MDOF system can be decomposed into the FRFs of each mode, and the influence of other modes on the mode of interest can be ignored. The natural frequency to be identified corresponds to the peaks of the FRF graph. However, the identification results are less precise in a system with high damping. In general, SDOF-based methods are only suitable for structures with separated natural frequencies and small damping ratios.

To overcome the drawbacks of SDOF-based methods, Richardson [11] introduced the Rational Fractional Polynomial (RFP) method to determine multiple modes simultaneously from the FRF. This method expresses the FRF as a fraction and uses the linear LS procedure of the error function between experimental and theoretical FRF measurements to estimate the coefficients of the FRF fraction. From

that, the natural frequencies can be calculated as the roots of the characteristic polynomial. The RFP has two important contents. First, the author converted the non-linear error function into a linear error function and therefore used a linear LS procedure (simple) instead of a non-linear LS procedure (complicated). Second, the author used the orthogonal polynomial function to overcome the degeneracy condition of the matrix when solving a system of linear algebraic equations. The advantage of the RFP method is that it can accurately determine modal parameters such as frequency, mode shape, and damping ratio, even in closely spaced modes. However, this method also has some limitations that when the mode has zero residue, the RFP method is less accurate [12]. Furthermore, this method requires knowing in advance the number of modes present in the measured data.

To improve the RFP method, Richardson [12] proposed the Global Rational Fraction Polynomial (GRFP) method which uses multiple FRF measurements simultaneously to determine dynamic characteristics such as damping ratios. However, like the RFP method, the GRFP method must manually determine the number of modes in the frequency band used. In many cases, it is impossible to determine the exact number of these modes from the FRF measurements. When the correct number of modes is not specified, the GRFP method can give false modes that are difficult to eliminate.

RFP and GRFP methods has been developed by many researchers [13-16]. In order to improve the accuracy of the GRFP method, the authors have also proposed a three-step procedure to automatically determine the modal parameters of structures [17]: Determine the number of modes in a frequency band

using a probability distribution density plot; compare and evaluate the nonlinear error between the identified FRF and the experimental FRF; finally, calculate the weighted average of the determined natural frequencies and damping ratios.

Modal analysis has been studied extensively worldwide. However, this field still faces many difficulties since engineering structures have a large number of DOFs, the damping mechanism and the influence of noise. In Vietnam, experimental tests and identification methods are attracting more and more attention in the field of research. Specifically, the authors have performed modal analysis for many structures by different methods such as Peak-Picking method [9], forced vibration method [18], Arduino platform [19] or Operational Modal Analysis [20]. Modal testing and structural identification are still being researched and developed.

The article develops the RFP method and uses the combined data in the frequency domain to determine the natural frequencies of structures. The combined data set is built on the basis of a random combination of initial measurement data. The convergence of identification results is determined by the frequency distribution density function. Numerical simulations of a 3-dof system with noise and an experimental test on a steel beam show the effectiveness of the proposed method.

2. Developing the rational fraction polynomial method

2.1 Rational fraction polynomial method

The theoretical frequency response function of a MDOF system can be expressed as a polynomial fraction.

$$H(\omega) = \frac{\sum_{j=0}^{2N-1} a_j (i\omega)^j}{\sum_{k=0}^{2N} b_k (i\omega)^k} = \frac{a_0 + a_1 (i\omega)^1 + a_2 (i\omega)^2 + ... + a_{2N-1}(i\omega)^{2N-1}}{b_0 + b_1 (i\omega)^1 + b_2 (i\omega)^2 + ... + b_{2N}(i\omega)^{2N}} \tag{1}$$

or

$$H(\omega) = \sum_{k=1}^{N} \left[\frac{r_k}{i\omega - p_k} + \frac{r_k^*}{i\omega - p_k^*} \right] \tag{2}$$

where N is the number of modes, $p_k = -\sigma_k + i\omega_k$ is the kth pole, ω_k is the kth angular frequency, r_k is the kth residue; r_k^*, p_k^* are the complex conjugates of r_k, p_k, respectively.

The RFP method was introduced by Richardson [11], based on the least square procedure of the error function between the theoretical and measured FRF to estimate the coefficients in (1).

$h_j = h(\omega_j)$ is assumed to be the value of the measured FRF at frequency ω_j. The error function

between the theoretical FRF and the measured FRF at frequency ω_j for m modes ($m \leq N$) is defined as follows:

$$\tilde{e}_j = \frac{a_0 + a_1(i\omega_j)^1 + a_2(i\omega_j)^2 + ... + a_{2m-1}(i\omega_j)^{2m-1}}{b_0 + b_1(i\omega_j)^1 + b_2(i\omega_j)^2 + ... + b_{2m}(i\omega_j)^{2m}} - h_j \tag{3}$$

Equation (3) is a non-linear function, and the LS procedure can be applied to estimate the coefficients. In order to simplify the estimation, the above equation can be converted to the following linear form (assuming $b_{2m}=1$):

$$e_j = [a_0 + a_1(i\omega)^1 + ... + a_{2m-1}(i\omega)^{2m-1}] - h_j[b_0 + b_1(i\omega)^1 + ... + b_{2m-1}(i\omega)^{2m-1}] - h_j(i\omega)^{2m} \tag{4}$$

Define an error vector (complex form) for s frequency points:

$$\{E\} = \{e_1 \quad e_2 \quad \cdots \quad e_s\}^T$$

Equation (4) can be deduced:

$$\{E\} = \begin{bmatrix} 1 & (i\omega_1)^1 & (i\omega_1)^2 & \cdots & (i\omega_1)^{2m-1} \\ 1 & (i\omega_2)^1 & (i\omega_2)^2 & \cdots & (i\omega_2)^{2m-1} \\ \vdots & \vdots & \vdots & \ddots & \vdots \\ 1 & (i\omega_s)^1 & (i\omega_s)^2 & \cdots & (i\omega_s)^{2m-1} \end{bmatrix} \begin{Bmatrix} a_0 \\ a_1 \\ \vdots \\ a_{2m-1} \end{Bmatrix} -$$

$$\begin{bmatrix} h_1 & h_1(i\omega_1)^1 & h_1(i\omega_1)^2 & \cdots & h_1(i\omega_1)^{2m-1} \\ h_2 & h_2(i\omega_2)^1 & h_2(i\omega_2)^2 & \cdots & h_2(i\omega_2)^{2m-1} \\ \vdots & \vdots & \vdots & \ddots & \vdots \\ h_s & h_s(i\omega_s)^1 & h_s(i\omega_s)^2 & \cdots & h_s(i\omega_s)^{2m-1} \end{bmatrix} \begin{Bmatrix} b_0 \\ b_1 \\ \vdots \\ b_{2m-1} \end{Bmatrix} - \begin{Bmatrix} h_1(i\omega_1)^{2m} \\ h_2(i\omega_2)^{2m} \\ \vdots \\ h_s(i\omega_s)^{2m} \end{Bmatrix} \tag{5}$$

or

$$\{E\} = [P]_{(s \times 2m)}\{a\}_{(2m \times 1)} - [T]_{(s \times 2m)}\{b\}_{(2m \times 1)} - \{W\}_{(s \times 1)} \tag{6}$$

The sum of squared errors depends on {a} and {b}:

$$J(\{a\}, \{b\}) = \sum_{j=1}^{s} e_j^* e_j = \{E^*\}^T \{E\} \tag{7}$$

The error function has a minimum value, the vectors {a}, {b} must satisfy:

$$\frac{\partial J}{\partial \{a\}} = 2\operatorname{Re}([P^*]^T[P]\{a\}) - 2\operatorname{Re}([P^*]^T[T]\{b\}) - 2\operatorname{Re}([P^*]^T\{W\}) = \{0\} \tag{8}$$

$$\frac{\partial J}{\partial \{b\}} = 2\operatorname{Re}([T^*]^T[T]\{b\}) - 2\operatorname{Re}([T^*]^T[P]\{a\}) + 2\operatorname{Re}([T^*]^T\{W\}) = \{0\} \tag{9}$$

Then {a}, {b} are determined from the following equations:

$$\begin{bmatrix} \operatorname{Re}([P^*]^T[P]) & -\operatorname{Re}([P^*]^T[T]) \\ \hline -\operatorname{Re}([T^*]^T[P]) & \operatorname{Re}([T^*]^T[T]) \end{bmatrix}_{(4m \times 4m)} \begin{Bmatrix} \{a\} \\ \hline \{b\} \end{Bmatrix}_{(4m \times 1)} = \begin{Bmatrix} \operatorname{Re}([P^*]^T\{W\}) \\ \hline -\operatorname{Re}([T^*]^T\{W\}) \end{Bmatrix}_{(4m \times 1)} \tag{10}$$

From the above equation, one gets {b} = {b_0 b_1 ... b_{2m-1}}^{T} and the natural frequencies are the roots of the characteristic equation:

$$f(i\omega) = b_0 + b_1(i\omega)^1 + b_2(i\omega)^2 + ... + b_{2m-1}(i\omega)^{2m-1} + (i\omega)^{2m} \tag{11}$$

2.2. Developing the rational fraction polynomial method

The RFP method offers the advantage to determine several natural frequencies from a single frequency domain data measurement. However, the RFP method also has limitations because when the residual r_k of a mode in the measured FRF data is zero, the characteristic polynomial will have no root

ω_k. Therefore, this method cannot determine the natural frequency ω_k. Even if r_k is relatively small compared to other residuals, the error of the identification procedure will be large due to the influence of noise.

In order to overcome the above limitation, the paper proposes to use combined measurements by adding the weighted average of the FRF measurements according to the formula:

$$H(\omega) = \frac{\sum_{j=1}^{n}\left(\delta_j H_j(\omega)\right)}{(\delta_1 + \delta_1 + ... + \delta_p)} = \frac{1}{(\delta_1 + \delta_1 + ... + \delta_p)}\sum_{j=1}^{n}\left(\delta_j \sum_{k=1}^{N}\left[\frac{r_{k(j)}}{i\omega - p_{k(j)}} + \frac{r_{k(j)}^*}{i\omega - p_{k(j)}^*}\right]\right) \qquad (12)$$

or

$$H(\omega) = \frac{1}{(\delta_1 + \delta_1 + ... + \delta_n)}\sum_{k=1}^{N}\left[\frac{\sum_{j=1}^{n}\left(\delta_j r_{k(j)}\right)}{i\omega - p_{k(j)}} + \frac{\sum_{j=1}^{n}\left(\delta_j r_{k(j)}^*\right)}{i\omega - p_{k(j)}^*}\right] \qquad (13)$$

where, δ_j is the weighted value of the jth FRF, n is the number of the FRF measurements.

Since the probability that any real number is zero is much smaller than the probability that the number is not zero. When the measured data has a residual $r_{k(j)}$ of zero, the probability that the sum $\sum_{j=1}^{n}\left(\delta_j r_{k(j)}\right)$ is zero is very small with a set of random weights $(\delta_1, \delta_2, ... \delta_n)$ such that $(\delta_1 + \delta_2 + ... + \delta_n) \neq 0$. This is the basis for proposing the process of determining the natural frequencies of the structure using synthetic measurement data. The procedure for the proposed method using combined measurement data is introduced as follows:

- Perform numerical simulation or experimental test to obtain *p* FRF measurement data;

- Generate average measurements FRF: H_{tb-1}, H_{tb-2}, …, H_{tb-n} corresponding to n sets of random weights $(\delta_1, \delta_2, ... \delta_n)$;

- For each measured data H_{tb-n}, calculate the vector {b} as the coefficients of the characteristic polynomial (10), and determine the natural frequencies which are the roots of the characteristic polynomial (11);

- Determine the probability density of the natural frequencies identified in the frequency range $\Delta\omega$;

- The final natural frequency is the average of the natural frequencies in the frequency range $\Delta\omega$ with a given probability.

3. Numerical simulation

3.1. Data simulation

Considering a 3-dof system with the natural frequencies, the damping ratios and the residuals r_k of the FRFs in (2) are given in Table 1. There are three measurements where each has a zero residue.

Table 1. *Simulation parameters of a steel beam*

Mode	Frequency (Hz)	Damping ratio (%)	Residue r_k		
			Measurement 1	Measurement 2	Measurement 3
1	10	5.0	3	5	0
2	20	3.0	0	2	4
3	40	4.0	2.5	0	1.5

Using the data in Table 1 to simulate three FRFs measurements. Noise is added to the signal using the inverse Fast Fourier Transforms of the theoretical FRFs to obtain IRFs; then, a random noise signal of constant amplitude is added to the IRFs; finally, the noisy IRFs are transformed into the noisy FRFs. Three FRF measurements in the frequency range [0-80] Hz with 3% noise are shown in Figure 1.
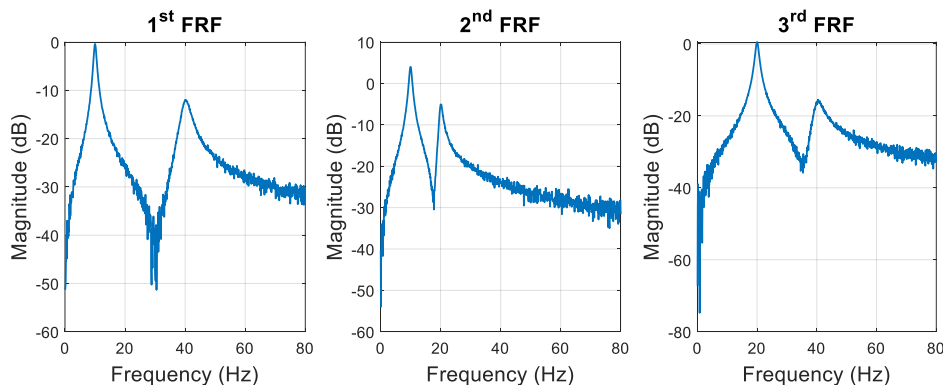

Figure 1. *The simulated FRFs of 3-dof system*

3.2. Identification from single measurements using the RFP method

Using the RFP method to determine the natural frequencies of the system with different frequency bands in the range [0 ÷ ω_{max}] Hz. Choosing the number of modes N=3 and the degree of the polynomial m=3. Changing the frequency range ω_{max}, the results of determining the natural frequencies by the RFP method for each measured data are presented in Tables 2, 3 and 4.

Table 2. *The natural frequency determined from the first measurement*

Mode	Theoretical frequency (Hz)	Identification in the frequency range [0 ÷ ω_{max}] (Hz)			
		[0 ÷ 50]	[0 ÷ 60]	[0 ÷ 70]	[0 ÷ 80]
1	10	9.9996	10.0015	10.0030	10.0094
2	20	---	---	---	---
3	40	39.9580	39.9939	40.0127	40.0445
---	---	44.0186	55.8087	65.0544	73.9851

Table 2 shows that only two modes (modes 1 and 3) can be identified. The second natural frequency cannot be identified because the residual of the second mode in the FRF measurement is zero. Instead, there is the appearance of frequencies far from the theoretical frequency but still in the frequency range of interest, so it is difficult to eliminate.

Table 3. *The natural frequency determined from the second measurement*

Mode	Theoretical frequency (Hz)	Identification in the frequency range [0 ÷ ω_{max}] (Hz)			
		[0 ÷ 50]	[0 ÷ 60]	[0 ÷ 70]	[0 ÷ 80]
1	10	10.0170	10.0667	10.1590	10.3704
2	20	20.1515	20.5380	21.4149	23.4233
3	40	45.5768	55.1039	63.7809	72.9300

Similarly, Table 3 also shows that the RFP method correctly recognizes only the first two modes, but the third mode gives a huge estimation error. Since the residue of the third mode is theoretically zero, when the measured data contains noise, this residue is relatively small compared to the other residue, causing this increase in this identification error.

Table 4. *The natural frequency determined from the third measurement*

Mode	Theoretical frequency (Hz)	Identification in the frequency range [0 ÷ ω_{max}] (Hz)			
		[0 ÷ 50]	[0 ÷ 60]	[0 ÷ 70]	[0 ÷ 80]
1	10	---	---	---	---
2	20	19.9961	20.0006	20.0001	20.0009
3	40	38.0073	39.9808	40.0717	40.2669
---	---	40.3279	55.4681	65.0835	74.0979

The results of natural frequencies determination in Tables 2, 3 and 4 all show that the frequency range significantly affects the accuracy of the results. Therefore, if the frequency band is closer to the resonant peak, the detected frequency will be more accurate. Far from the resonant peak, there is often significant noise in the high-frequency domain, so the identification error is high. In Table 3, with the frequency range [0÷80] Hz, the second natural frequency identification error is up to 17% (23.4 Hz compared to 20 Hz).

Therefore, narrowing the frequency range is an effective way to reduce the estimation error of natural frequencies. However, since the structure's natural frequency is unknown, it is sometimes difficult to reduce this frequency range.

3.3. Identification from combined measurements

Performing the identification procedure as in section 2.2, with three noise FRF measurements. Create sets of random weights (δ_1, δ_2, … δ_n) and calculate the synthesis measurements according to (13), and then estimate the natural frequencies of the structure in the range frequency [0 ÷ ω_{max}] with limited frequency ω_{max} = 80 Hz. The results of determining the natural frequency with 50 sets of synthetic measurement data are shown in Figure 2(a) and the

distribution densities of the identified natural frequencies are shown in Figure 2(b). Accordingly, the estimated frequencies are indicated by signs "+", frequencies located in the vicinity of ±0.5 Hz compared to the natural frequencies in Table 1 are marked with a circle.
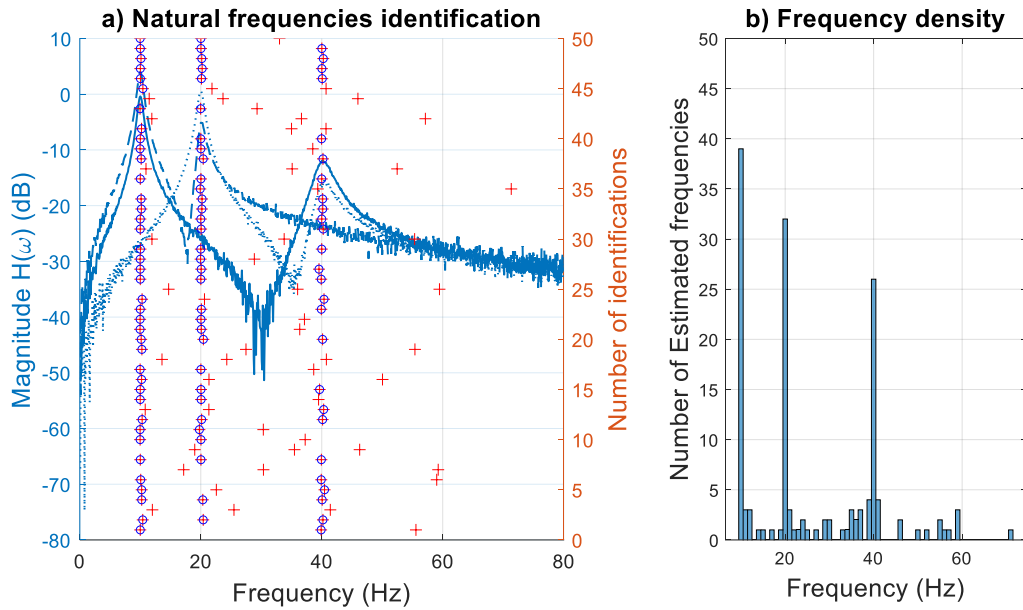

Figure 2. *Natural frequencies estimated from combined data, (n=50)*

From Figure 2(b), it can be seen that there are three modes identified with densities above 50%. The specific values of the natural frequency and the corresponding density are shown in Table 5. The final frequency value is the average of the frequencies in the range $\Delta\omega = 1$ (Hz).

Table 5. *The natural frequency identified from combined measurements, (n=50)*

Mode	Theory	Identification	Error (%)	Density (%)
1	10	10.0823	0.82	78
2	20	20.0904	0.45	64
3	40	40.0609	0.15	52

Increasing the combined measurement data set to 100 and narrowing the range of recognized frequencies to the range $[0 \div \omega_{max}]$ with a limited frequency $\omega_{max} = 55$ Hz. The results of determining the natural frequencies are shown in Figure 3 and Table 6.
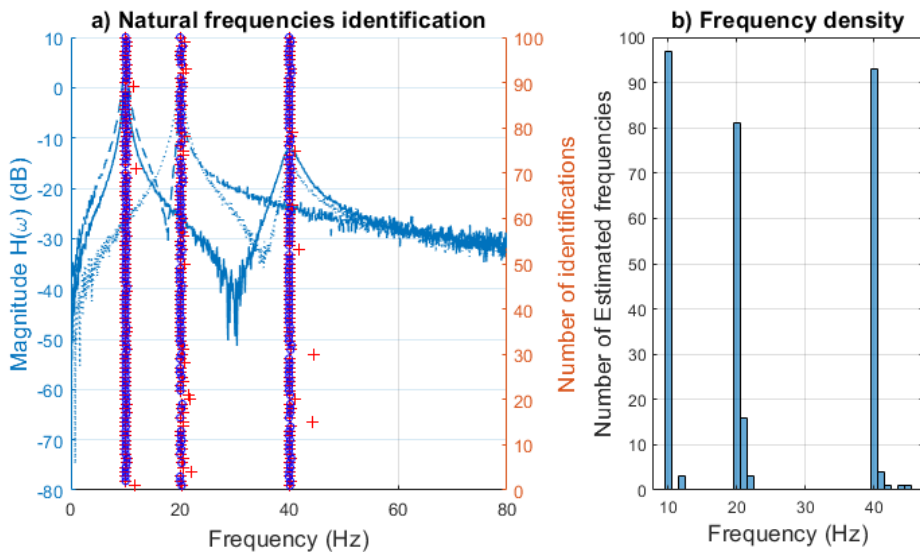

Figure 3. *Natural frequencies estimated from combined data, (n=100)*

Tables 5 and 6 show that, when narrowing the frequency band, the probability of determining natural frequencies increases by more than 80%, and the identified natural frequencies are also quite accurate (less than 1% error). Therefore, using the measured data in combination with the frequency density function allows to accurately determine all three natural frequencies of the structure simultaneously.

Table 6. *The natural frequency identified from combined measurements, (n=100)*

Mode	Theory	Identification	Error (%)	Density (%)
1	10	10.0769	0.77	97
2	20	20.1654	0.83	81
3	40	40.1204	0.30	93

4. Experimental test
4.1 Structure and experimental instruments

The experimental structure is a steel cantilever beam with the following physical parameters:

Table 7. *Physical parameters of the steel cantilever beam*

Parameter	Value	Unit
Length, L	710	mm
Width, b	60	mm
Height, h	8	mm
Elastic modulus, E	2.03E+5	N/mm^2
Mass density, ρ	7850	kg/m^3

The SCXI-1000DC measurement system, LabVIEW software, an impact hammer PCB 086C03 and an accelerometer PCB 352C68 were used in the test. They are shown in Table 8.

Table 8. *Experimental software and equipment*

Name	Model (Company)	Range (sensivity)
Hammer	PCB 086C03 (PCB Piezotronics, Inc)	±2224N (2.25mV/N)
Accelerometer	PCB 352C68 (PCB Piezotronics, Inc)	±50g (100mV/g)
Measurement system	NI SCXI-1000DC (National Instruments)	Multi-channel
Software	LabVIEW 2011 (National Instruments)	

4.2. Experimental scheme and procedure

The experimental scheme is shown in Figure 4. A computer uses LabVIEW software connected to the measurement system NI SCXI-1000DC. The measurement system connects to the impact hammer PCB 086C03 and accelerometer PCB 352C68 (mounted at the free end of the beam).
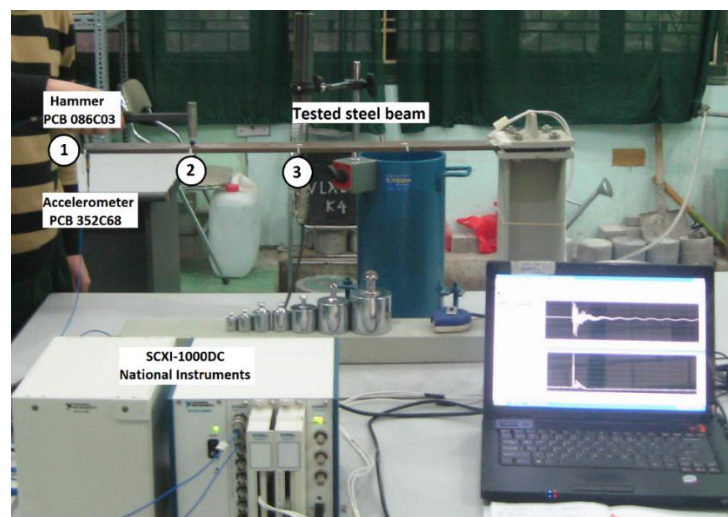

Figure 4. *Experimental test*

The beam is divided into four equal sections. Using a force hammer to hit positions 1, 2 and 3. The impact force and acceleration are automatically recorded by computer software over time. FRF measurements can also be calculated automatically in LabVIEW or using the FFT in MATLAB. The magnitude plots of these FRFs are shown in Figure 5.
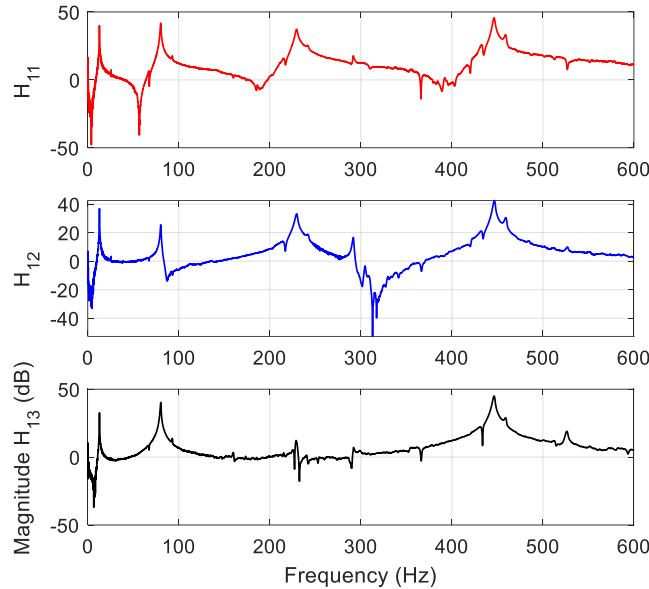

Figure 5. *Magnitudes of the measured FRFs*

It can be seen from Figure 5 that H_{11} has four distinct resonance peaks, H_{12} can have from 5 to 6 resonance peaks, and H_{13} has only three distinct resonance peaks. This is challenging for identification methods based on SDOF or single measurement data.

4.3. Identification from single measurement

Using the RFP method with the measured data H_{13} to determine the natural frequencies of the system with different frequency bands in the range [0 ÷ ω_{max}] Hz. Changing the frequency ω_{max}, the identification results of natural frequencies by the RFP method for each measured data are shown in Figure 6(a). The estimated frequencies are indicated by the sign "+", and adjacent frequencies within 5% on either side of the resonant frequency are marked with a circle. The corresponding frequency density graph is shown in Figure 6(b).
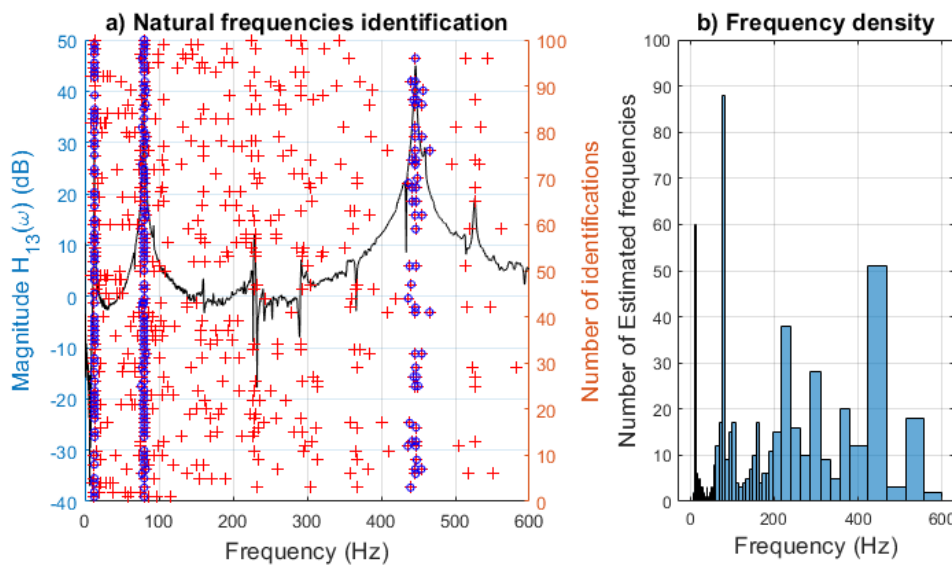

Figure 6. *Natural frequencies determined from the measured data H_{13}*

It can be seen from Figure 6 that H_{13} has only three distinct resonance peaks, so only three natural frequencies (1, 2 and 4) are identified with a probability density higher than 50%. The third mode is not identified or is a suspicious mode with a relatively low probability (only 38%).

4.4. Identification from combined measurement

Similar to section 3.3, combined measurement data sets are created to determine the natural frequencies of the beam with different frequency bands in the range $[0 \div \omega_{max}]$ Hz. Based on 100 sets of synthetic measurement data, the results of determining the natural frequencies and the corresponding frequency distribution density are shown in Figure 7.
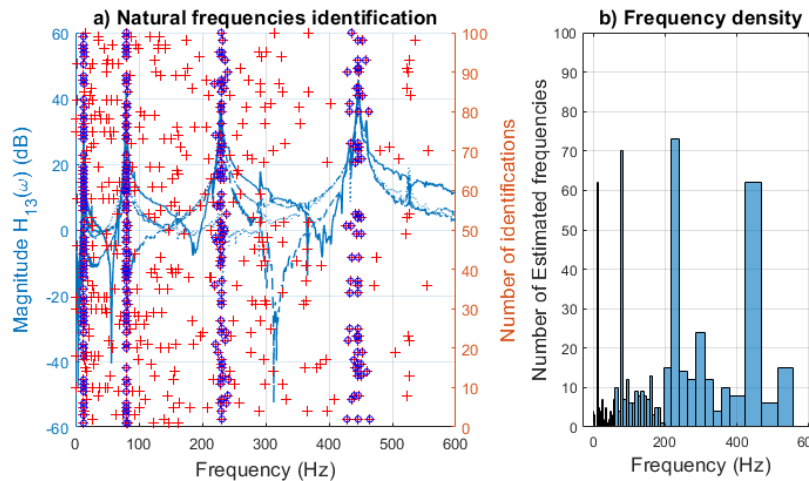

Figure 7. *Natural frequencies determined from combined data*

Figure 7(b) shows that all four natural frequencies are identified with densities above 60%. Table 9 presents the identification results by the RFP method for the single measurement data H_{13} and the proposed procedure for the combined measurement data. The RFP method using a single measured data H_{13} identifies only three frequencies with the densities of identified frequencies less than 50%. Meanwhile, the procedure proposed in this paper with synthetic measurement data can determine all four natural frequencies with minor errors compared to the results obtained from the finite element model.

Table 9. *The comparison of identification results*

Mode	Frequencies from finite element model	RFP method with a single measured data H_{13}		Proposed procedure with combined measurement data		Error (%)
		Frequency	Density (%)	Frequency	Density (%)	
1	13.0	12.97	60	12.94	62	0.45
2	81.7	79.94	88	80.37	70	1.63
3	228.8	--------	38 (small)	230.16	73	0.60
4	448.3	446.60	51	444.10	62	0.94

5. Conclusion

This paper develops the RFP method to identify the natural frequencies of structures by building and using the combined measurement data in the frequency domain and the frequency density function. The numerical simulations of the 3-dof system and the experimental test of the steel beam have shown that the proposed procedure is effective when the measured data for a certain mode has a relatively small or zero residue. The natural frequencies identified from the steel beam are compared with that obtained from the finite element model with small error. This validates the reliability of the experiment and the calculated results.

REFERENCES

[1] Ibrahim S. R. (1977). Random Decrement Technique for Modal Identification of Structures. *Journal of Spacecraft and Rockets, 14 (11), pp. 696-700.*

[2] Spitznogle F. R., Quazi A. H. (1970). Representation And Analysis Of Time-Limited Signals Using A Complex

Exponential Algorithm. *The Journal of The Acoustical Society of America, Vol. 47, No. 5 (Part I), pp.1150-1155.*

[3] Brown D. L., Allemang R. J., Zimmerman R., Mergeay M. (1979). Parameter Estimation Techniques For Modal Analysis. *SAE Technical Paper Series, No. 790221.*

[4] Ewins D. J. (2000). Modal Testing: Theory, Practice, and Application, 2nd ed., *Research Studies, New York, Chap 3, 4.*

[5] Guo Z., Sheng M., Ma J., Zhang W. (2015). Damping identification in frequency domain using integral method. *Journal of Sound and Vibration 338, pp. 237-249. DOI:10.1016/j.jsv.2014.10.040.*

[6] Nguyễn Tiến Khiêm, (2008). Nhập môn Chẩn đoán kỹ thuật công trình, *NXB KHTN&CN, Hà Nội.*

[7] Đào Như Mai (2005), Độ nhạy cảm của các đặc trưng động lực học kết cấu và ứng dụng trong chẩn đoán kỹ thuật công trình, *Luận án tiến sĩ kỹ thuật, Viện Cơ học, Hà Nội.*

[8] Vu Dinh Huong (2022). Experimental identification of Caughey and Rayleigh viscous damping matrices of steel beam structures, *Journal of building science and technology – 2/2022, pp. 12-20.*

[9] Vũ Đình Hương, Lê Anh Tuấn, Nguyễn Tương Lai (2015). Thí nghiệm nhận dạng các tham số tần số và cản của kết cấu tháp điện gió trên quần đảo Trường Sa. *Hội nghị Khoa học toàn quốc Cơ học Vật rắn biến dạng lần thứ XII, Đại học Duy Tân, TP Đà Nẵng, 7/8/2015.*

[10] Torvik P. J. (2011). On estimating system damping from frequency response bandwidths. *Journal of Sound and Vibration 330, pp. 6088-6097.*

[11] Richardson M. H. & Formenti D. L. (1982). Parameter Estimation from Frequency Response Measurements using Rational Fraction Polynomials, *Proceedings of the 1st IMAC, Orlando, Florida, pp. 1-15.*

[12] Richardson M. H. & Formenti D. L. (1986). Global Frequency and Damping from Frequency Response Measurements, *Proceedings of the 4th IMAC, Los Angeles, California, pp. 1-7.*

[13] Friswell, Michael & Penny, John. (1993). The choice of orthogonal polynomials in the rational fraction polynomial method. *Modal Analysis. 8. 257-262.*

[14] Carcaterra, A., D'Ambrogio, W. (1995). An iterative rational fraction polynomial technique for modal identification. *Meccanica 30, 63–75. DOI:10.1007/BF00987126.*

[15] Omar, Omar & Tounsi, Nejah & Ng, Eu-Gene & Elbestawi, Mohamed. (2010). An optimized rational fraction polynomial approach for modal parameters estimation from FRF measurements. *Journal of Mechanical Science and Technology. 24. 831-842. DOI:10.1007/s12206-010-0123-z.*

[16] N. Pandiya and W. Desmet. (2022). Direct estimation of residues from rational-fraction polynomials as a single- step modal identification approach. *Journal of Sound and Vibration, vol. 517, article 116530.*

[17] Vũ Đình Hương và Tạ Đức Tuân (2017). Nâng cao độ chính xác của phương pháp RFP nhận dạng tỷ số cản nhớt của kết cấu công trình. *Hội nghị Cơ học toàn quốc lần thứ X, Hà Nội, 8-9/12.*

[18] Tạ Đức Tuân, TS. Lê Anh Tuấn, TS. Vũ Đình Hương (2017). Nhận dạng tần số dao động riêng của kết cấu bằng phương pháp kích động cưỡng bức, *Tạp chí KHCN Xây dựng – số 1.*

[19] Ta Duc, Tuan., Le Anh, Tuan., Vu Dinh, Huong. (2018). Estimating Modal Parameters of Structures Using Arduino Platform. In: Nguyen-Xuan, H., Phung-Van, P., Rabczuk, T. (eds) Proceedings of the International Conference on Advances in Computational Mechanics 2017. ACOME 2017. Lecture Notes in Mechanical Engineering. *Springer, Singapore. DOI: 10.1007/978-981-10-7149-2_76.*

[20] Tran, Trung Duc and Le, Anh Tuan and Vu, Dinh Huong (2021). Identification Vibration Characteristics of Structures by Operational Modal Analysis (OMA) Technique. In: 24th International Scientific Conference on Construction: The Formation of Living Environment, *FORM 2021, 22 April 2021 through 24 April 2021, Moscow. DOI: 10.1007/978-3-030-79983-0_39.*